

Article

# Thermal Characterization of *Pinus radiata* Wood Vacuum-Impregnated with Octadecane

Rodrigo Fuentes-Sepúlveda <sup>1</sup>, Claudio García-Herrera <sup>1</sup>, Diego A. Vasco <sup>1,\*</sup>,  
Carlos Salinas-Lira <sup>2</sup> and Rubén A. Ananías <sup>3</sup>

<sup>1</sup> Departamento de Ingeniería Mecánica, Universidad de Santiago de Chile, Avda. Lib. Bdo. O'Higgins 3363, 9170002 Santiago, Chile; rodrigo.fuentess@usach.cl (R.F.-S.); claudio.garcia@usach.cl (C.G.-H.)

<sup>2</sup> Departamento de Ingeniería Mecánica, Universidad del Bío-Bío, Avda. Collao 1202, Casilla 5-C, 4030000 Concepción, Chile; casali@ubiobio.cl

<sup>3</sup> Departamento de Ingeniería en Maderas, Universidad del Bío-Bío, Avda. Collao 1202, Casilla 5-C, 4030000 Concepción, Chile; ananias@ubiobio.cl

\* Correspondence: diego.vascoc@usach.cl; Tel.: +56-(0)2-271-83120

Received: 3 December 2019; Accepted: 19 December 2019; Published: 20 February 2020



**Abstract:** The incorporation of phase change materials (PCM) in construction components has become an alternative to reduce the effect of thermal loads in buildings with low thermal inertia. This study put together the effective heat storage capacity of an organic phase change material (O-PCM, octadecane) with the construction and production potential of *Pinus radiata* in Chile. The wood is impregnated with octadecane by using the Bethell method, showing that it has good retention of the impregnator, and that its size was not modified. Differential scanning calorimetry analysis (DSC) showed that the composite material could achieve fusion enthalpy values from 36 (20.8 MJ/m<sup>3</sup>) to 122 J/g (108.9 MJ/m<sup>3</sup>). The transient line heat source method used, indicated that impregnation of *Pinus radiata* with octadecane increases its specific heat at temperatures from 15 to 20 °C, while its thermal conductivity decreases in the radial and the tangent directions, and increases in the longitudinal direction, showing a decrease in the orthotropic behavior of the wood. The ability of *Pinus radiata* wood to store latent heat positioned it as a candidate material to be considered in the building industry as a heat storage system.

**Keywords:** *Pinus radiata*; impregnation; octadecane; thermal properties

## 1. Introduction

Chile's commercial, public and residential sectors consume 22% of the total energy produced (64,814 Tcal in 2017) [1], and approximately 80% of this energy is consumed by the residential sector [2]. In this sector approximately 56%–62% of the total energy is used for generation of heat by using wood, positioning wood as the main source of energy for this purpose (80%) [3]. The intensive use of wood for heating has created several environmental problems, especially at the south of the country. The Chilean policy for the use of firewood for heating establishes, among other strategies, the need for more efficient building isolation, given that only 35% of Chilean's homes have energy efficient systems. Some of the guidelines from this policy are the promotion of new isolation construction technologies and, development of new energy efficient building systems [4].

The storage of thermal energy using phase change materials (PCM) has been recommended as a technological alternative to increase energy efficiency in buildings [5]. One of the main effects of the high thermal storage capacity of PCM is the increase of the thermal inertia of the building materials, which helps to regulate inside room temperature. The study of PCM integration methods in building materials started by using direct incorporation methods, such as imbibing [6,7], a technique that

consists of immersing the building materials, such as gypsum boards, bricks or concrete blocks, in PCM baths, where the PCM is absorbed within the material pores and cavities. Moreover, there is a possibility of direct incorporation of PCM within structures or materials building, which is known as the shape-stabilized PCM method [8]. In this material, PCM can retain the shape of the solid structure during phase transition. A shape-stabilized PCM is a composite of PCM with another material. The most important benefits of shape-stabilized PCM are [9]: (i) apparent heat capacity comparable to other PCM; (ii) suitable overall thermal conductivity; (iii) good compatibility with building envelope materials; (iv) the carrier material can serve as a structural component of building envelopes and (v) there is no need for encapsulation if the PCM does not tend to flow out of the porous structure during melting.

Chile is an important player in wood production, with 8.15 million cubic meters, 96.9% of which is obtained from *Pinus radiata* pine species, a versatile, fast-growing, medium-density softwood, suitable for a wide range of uses. In terms of relative economic importance, the forest sector in Chile has occupied historically the second and third place in export participation [10]. According to Chilean National Institute of Statistics (INE), around 17% of the houses in the country are built with wood as the structural material [11], and only 13% of the new homes, built in 2016, used wood as a predominant material [12]. Currently, only in the coastal area and in the southern regions of the country, the use of wood as a building material for housing has significant activity, mainly because of the humid and cold weather conditions and closeness to forest areas. In recent years, wood has been extensively used as a building material for social housing supported by government's subsidies [13]. In Chilean context, *Pinus radiata* is the most suitable material for different types of construction. It is used mainly for wall separation, beams, structures and other applications, where the precision of the dimensions and finishing is required: roof cover and base of floor, interior division and panel construction [14].

Wood is a porous, heterogeneous and hygroscopic material. The wood heterogeneity and anisotropy are consequence of its anatomical characteristics, given that its cell constitution can be of variable nature and shape. Therefore, the anatomical properties of wood should have an important effect on transport processes such as impregnation. Permeability is a physical property defined as the ability of porous media to transport fluids. The radial permeability of *Pinus radiata* grown in Chile is lower than the tangential permeability [15], which is explained by the bigger pits and their disposition mainly on radial cell-walls of early tracheids. Impregnation of wood is defined as a method that results in the filling of the wood substance with an inert material (impregnant) in order to have a desired performance change. The molecular components of the impregnant should be small enough; so they can access to the inside of the cell wall, and it is essential that the impregnant be non-leachable under service conditions [16].

There are few studies addressing impregnation by PCM using wood as a substrate. In 2016, Li et al. [17] impregnated green fir wood with an aqueous solution of polyethylene glycol (PEG) at atmospheric pressure. They obtained a composite with melting and freezing point capabilities of 26.74 °C and 36.14 °C, respectively, and a latent heat of 73.59 J/g. They applied a surface coating to avoid leakage of the PCM and conducted leaching and thermal stability tests. Barreneche et al. [18] impregnated black alder wood with paraffinic PCM RT-21 and RT-27 from Rubitherm® (Berlin, Germany), by applying vacuum. The authors measured a latent heat range of 2.41–20.62 J/g for a weight fraction of PCM of 10.5%–29.9%, respectively. The authors applied a polystyrene solution to prevent any leakage when the PCM was in a liquid state. In 2018, Vasco et al. [19] studied the kinetics of the impregnation process of *Pinus radiata* wood with reagent grade octadecane at four manometric pressures (0–3 bar) and a constant temperature of 50 °C. The authors obtained a composite with a maximum final octadecane content of 65.5%, and showed that the impregnation process is possible, verifying that both the thermal conductivity and the enthalpy of the wood improved. However, they found that leakage of octadecane is an issue during its melting. Recently, Mathis et al. [20] impregnated two species of hardwood (red oak and sugar maple) with a micro-encapsulated PCM to improve the thermal inertia of wood boards for floor usage. The authors reported heat storage improvement of 77.0%

and 7.1% for red oak and sugar maple, respectively. Recently, Montanari et al. [21] obtained transparent wood (TW) with latent heat storage capacity (76 J/g). The characterization of the performance of thermal energy regulation showed that the prepared TW-TES compound is better than regular glass due to the combination of heat storage and thermal insulation properties.

This study aims to analyze the effect on the thermal properties of *Pinus radiata* wood due to impregnation under vacuum with technical grade octadecane. The main contributions of this study are the thermal characterization of vacuum impregnated *P. radiata* wood with octadecane according to the temperature and the anatomical orientation of the wood. One expects that the anatomical orientation has a significative effect on PCM impregnation and thermal properties. We also aim to analyze the distribution of PCM in the porous wood structure by estimating the phase change enthalpy in each anatomical direction. In general, the impregnated wood acquires a thermal behavior like that of the pure impregnant (octadecane).

## 2. Materials and Methods

### 2.1. Materials

*Pinus radiata* wood comes from Yumbel city, Chile (72°36'57.42 longitude, 37°5'18.17 south latitude). The sample are made in slices of cylindrical shape, according to Chilean standard NCh631:2003 [22] (Figure 1). The humidity content of the samples is 12%, corresponding to the dry wood condition. The impregnant used is technical grade octadecane with purity of 90% provided by Gute Chemie [23], belonging to the family of paraffinic phase change materials. The main referential properties of wood and octadecane are presented in Table 1. Furthermore, a hardening epoxy resin coating was used to reduce the percolation problems of impregnated wood at temperatures higher than the melting temperature of the PCM (26 °C). Only those impregnated wood samples were coated with epoxy resin.

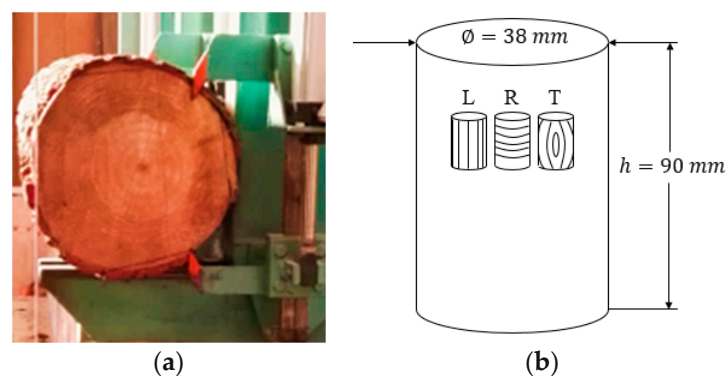


**Figure 1.** Obtaining samples: (a) cross section of the log. (b) Sample dimensions and anatomical directions. L: longitudinal, R: radial, T: tangential.

**Table 1.** Thermophysical characteristics of the impregnant [23] and *Pinus radiata* wood properties.

| Property                        | O-PCM (Octadecane Technical Grade) | Drywood (Radiata Pine) |
|---------------------------------|------------------------------------|------------------------|
| Molecular weight (g/mL)         | 254                                | -                      |
| Density (kg/m <sup>3</sup> )    | 780                                | 388                    |
| Melting temperature (°C)        | 26                                 | -                      |
| Boiling point (°C)              | 316                                | -                      |
| Flash point (°C)                | 154                                | -                      |
| Conductivity (W/m °C; 22 °C)    | 0.594                              | 0.311                  |
| Specific heat (kJ/kg °C; 22 °C) | 4660                               | 1818                   |
| Heat of fusion (kJ/kg)          | 133.20                             | -                      |

## 2.2. Methodology

### 2.2.1. Impregnant Characterization

Initially, the thermal conductivity and heat capacity properties of the impregnator were determined by using a transient line heat source and calorimetry methods, respectively. Specifically, through the thermal properties analyzer KD2 Pro (DECAGON) and the SH-1 probe, the thermal conductivity and the volumetric specific heat in the solid phase were obtained, and with the KS-1 probe the thermal conductivity in the liquid phase was determined, while the specific heat of this phase was determined from a calorimeter device. The experimental setup for transient line heat source method (KD2 Pro) is presented in Figure 4. A similar setup was used for the thermal characterization of wood impregnated with PCM.

The setup for the determination of PCM heat capacity in the liquid phase consisted of a calorimeter containing the PCM (Figure 2), which was stirred with a magnetic stirrer (Hanna Instruments, model HI 190M), to keep PCM temperature homogeneous. Heat flux is generated by means of an electrical resistor, which was subjected to a controlled voltage power supply through a direct current generator (QW, model QW-MS305D). The temperature increase rate was obtained through a K-type thermocouple (Chromel–Aluminum joint) immersed in the calorimeter, and through a data acquisition system (National Instruments, model NI cDAQ-9174). PCM mass was obtained by means of an analytical balance (Radwag, model WLC 6/F1/R).

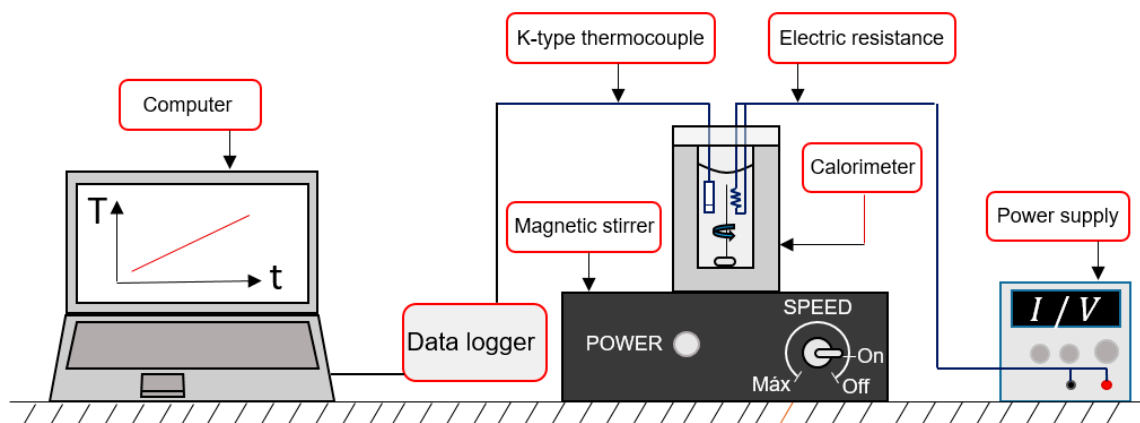


**Figure 2.** Measurement of heat capacity for impregnant (technical grade octadecane).

### 2.2.2. Impregnation Method

The impregnation method is based on the Bethell process [24]. In particular, the impregnation is carried out by immersing the wooden samples in a vessel containing the liquid octadecane, and then introducing it in a vacuum oven (Labtech, model LDO-080F) at 60 °C, to keep the pores of the wood dilated and PCM in a liquid state (Figure 3a). The impregnation process is carried out in three stages (Figure 3b), first an initial vacuum pressure of 85 kPa was applied for 20 min by means of a vacuum pump (Rocker 400) to extract the air from the porous matrix of the wood and increase the impregnation potential, second, the vacuum pressure was released, and the sample was kept at atmospheric pressure for 45 min during this time PCM impregnated the porous structure of the wood. Third, a vacuum stage of 40 kPa was applied for 10 min, to avoid the recoil effect and the percolation of impregnant through the surface of the wood. This stage was commonly used with water-based preservatives, when the wood samples were not immersed in the impregnant. Once the impregnation was finished, the wooden specimens were removed and dried with paper towels, to measure the retention of wood samples after

impregnation with octadecane, maintaining wood samples temperature under the melting point. The calculation formula is:

$$PCM \text{ retention} = \frac{W_{\text{impregnated wood}} - W_{\text{dry wood}}}{V_{\text{dry wood}}}, \quad (1)$$

where  $W_{\text{impregnated wood}}$  is the mass of impregnated wood,  $W_{\text{dry wood}}$  is the mass of unimpregnated wood and  $V_{\text{dry wood}}$  is the volume of unimpregnated wood. To study the effect of impregnation on dimensional variation of wood, and thus normalize the increase in mass by impregnation on a volumetric basis, we measured the diameters and heights of each wood sample. Given the dimensional variability of wood compared to more rigid materials, two diameters are measured at three levels of height using a caliper (Mitutoyo, model 500-144) for the subsequent calculation of a representative average diameter. In the same way we proceeded with the height measurement, then weighed each sample with a precision balance (Radwag, model WLC 6/F1/R). After 6 h of exposure of two tangential wood samples to temperatures above PCM melting point (35 °C), it was observed that mass loss of PCM due to percolation is on average 1.5% (Table 2).

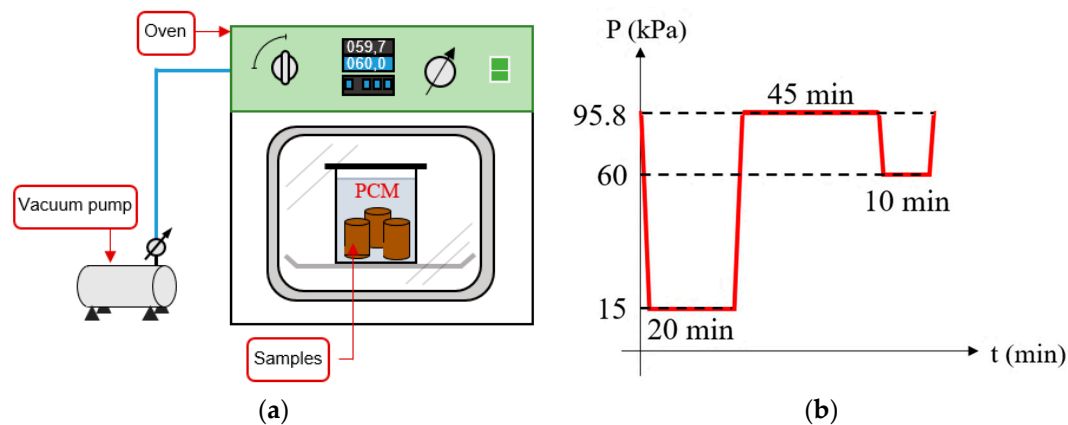


**Figure 3.** Schematics of (a) wood impregnation process in a vacuum oven, and (b) stages of the modified Bethel process.

**Table 2.** Mass loss of impregnated wood samples after 6 h at 35 °C.

| Sample       | Initial Mass (g) | Final Mass (g) | Weight Loss (%) |
|--------------|------------------|----------------|-----------------|
| Tangential 1 | 96.5883          | 95.0775        | 1.56            |
| Tangential 2 | 85.5112          | 84.3338        | 1.38            |

### 2.2.3. Thermal Characterization of *Pinus radiata* Wood Impregnated with Octadecane

The properties of thermal conductivity and volumetric specific heat of the impregnated *Pinus radiata* wood were determined, considering PCM in solid state (5–20 °C) and in the liquid state (30–35 °C) within the impregnated wood. Thermal properties of the unimpregnated wood were considered constant in the analyzed temperature range and were measured at 25 °C. Samples in the three directions (longitudinal, radial and tangential) were considered. For each direction there were five samples, both impregnated and unimpregnated samples. The temperature control was made by means of water recirculation, using a thermoregulated bath (Ron-Fong Technology, model BL-20), inside a double-jacketed container where the cylindrical wooden sample were placed, filling the remaining spaces with thermal paste. To achieve a better controlled environment, the sample was placed in an acrylic vessel, to reduce the effect of external humidity, a plastic film was used to seal the vessel with a layer of silica gel. The temperature and humidity of the sealed vessel were measured with a Testo 174H data logger (Figure 4).

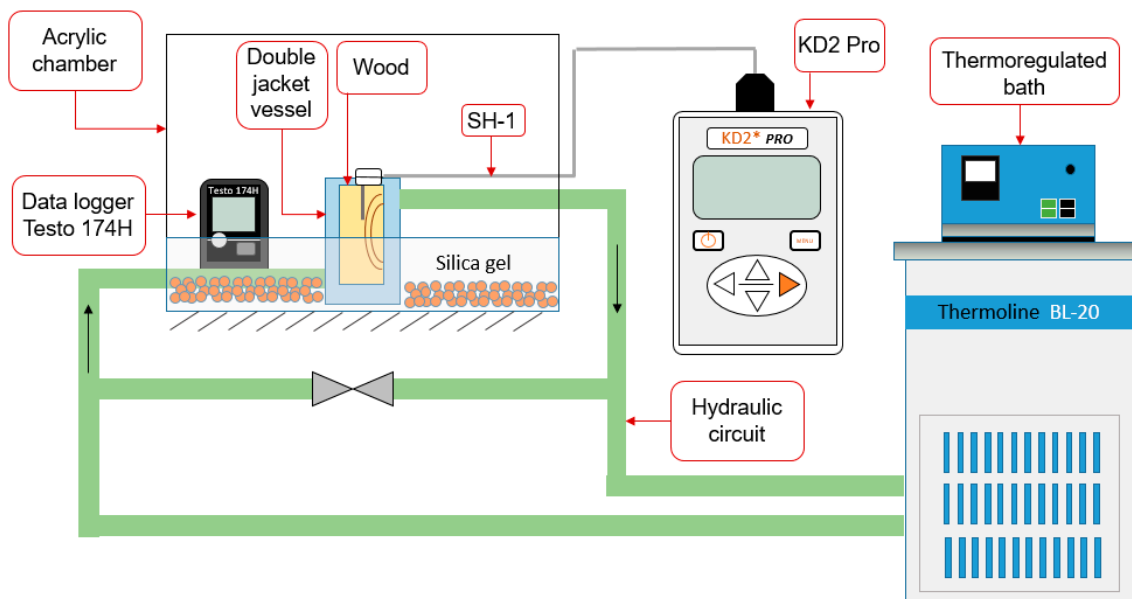


**Figure 4.** Experimental setup for thermal characterization of phase change material (PCM)-impregnated *Pinus radiata* wood.

#### 2.2.4. Phase Change Enthalpy Determination

The phase change enthalpy of the impregnated wood and the impregnator was determined through a differential scanning calorimetry (DSC 4000 System, PerkinElmer). Disc-shaped cuts (3 mm thick) were made with a punching tool, from the impregnated wood specimens at three different equidistant positions (Figure 5a). Three samples were obtained from each of the three disc-shaped cuts: one in the center, and two at 8 mm from the ends, as indicated in Figure 5b. The samples were then sanded to an average thickness of 0.5 mm, to be weighed in an analytical balance with  $\pm 0.01$  mg accuracy (Radwag, model AS 82/220.R2) and arranged in 40  $\mu\text{L}$  aluminum crucibles for characterization, so that the diameter of the samples covered the base of the crucibles, as much as possible. The average mass of the samples for longitudinal, radial and tangential directions were  $12.66 \pm 1.18$  mg,  $14.63 \pm 1.50$  mg and  $12.43 \pm 1.54$  mg, respectively, and PCM of  $13.11 \pm 2.27$  mg.

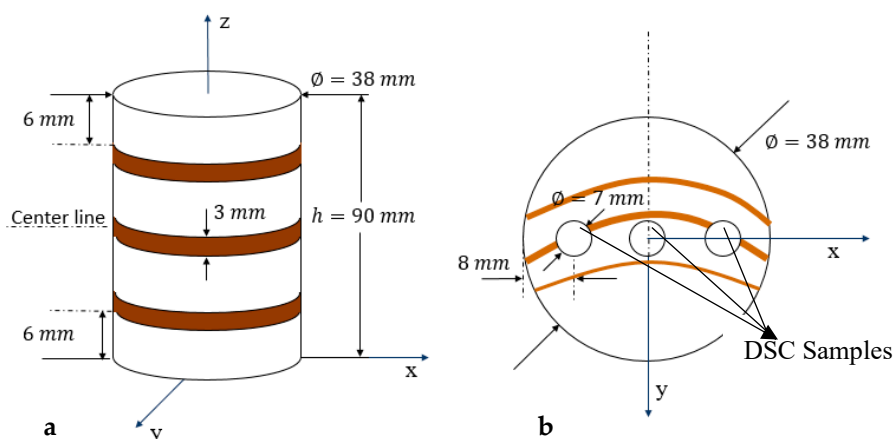


**Figure 5.** Samples for differential scanning calorimetry (DSC) taken from the impregnated wood specimens. (a) Disc-shaped cuts of a sample and (b) DSC samples from each disc-shaped cut.

For DSC analysis ( $\text{N}_2$  atmosphere of 20 mL/min) of PCM and impregnated wood samples, a dynamic method was used, maintaining an initial temperature of 10  $^\circ\text{C}$  for 10 min, and then heating

the samples at a rate of 1 °C/min until a temperature of 40 °C, that was maintained for 10 min. Then, the samples were cooled down to 10 °C at a rate of 1 °C/min, to finally keep the sample at 10 °C for 10 min, as shown in Figure 6. The relatively high heating and cooling rates obeyed to the restricted capabilities of the DSC. It is known that PCMs require a lower heating rate (0.1 °C/min) to obtain more accurate situation [25]. To diminish the effect of the mass sample, one increased the time of thermal equilibrium to 10 min in the DSC program. Moreover, it is important to mention here that the DSC technique was used to assess the distribution of PCM in the porous network of wood. Table 3 shows a summary of the experimental procedures with wood samples.

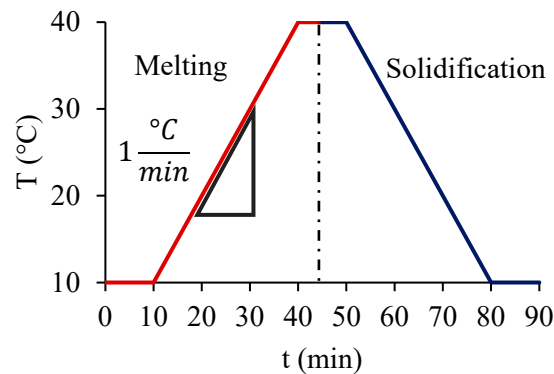


**Figure 6.** Temperature control for the DSC analysis.

**Table 3.** Summary of the experimental procedures with wood samples (TLHS: transient line heat source method).

| Anatomical Direction | Impregnation | Coating | Retention Test Samples | Thermal Characterization (TLHS) |             | DSC     |             |
|----------------------|--------------|---------|------------------------|---------------------------------|-------------|---------|-------------|
|                      |              |         |                        | Samples (38 mm × 38 mm × 90 mm) | Repetitions | Samples | Repetitions |
| Longitudinal         | Y            | Y       | 5                      | 5                               | 5           | 9       | 1           |
|                      | N            | N       | 0                      | 3                               | 5           | -       | -           |
| Radial               | Y            | Y       | 5                      | 5                               | 5           | 9       | 1           |
|                      | N            | N       | 0                      | 3                               | 5           | -       | -           |
| Tangential           | Y            | Y       | 5                      | 5                               | 5           | 9       | 1           |
|                      | N            | N       | 0                      | 3                               | 5           | -       | -           |

### 3. Results

#### 3.1. Impregnation

The change of size of wood samples, before and after the impregnation with octadecane, was not significant for PCM in liquid and solid states. The dimensional variation, due to the effects of the impregnation with octadecane, did not exceed 0.5% in the three directions (Table 4).

**Table 4.** Dimensional variation of wood samples after impregnation with octadecane.

| Anatomical Direction | Dimensional Variation (%) |
|----------------------|---------------------------|
| Longitudinal         | $-0.01 \pm 0.13$          |
| Radial               | $0.03 \pm 0.22$           |
| Tangential           | $0.35 \pm 0.19$           |

According to the results shown in Figure 7, the increase of retention after impregnation was  $449 \pm 98 \text{ kg/m}^3$  ( $115\% \pm 25\%$ ), average. To analyze the retention capacity of PCM by the porous structure of the wood, the retention decrease of 14 wood samples in the longitudinal direction, after keeping them one day at ambient temperature, was measured showing a decrease of  $0.136 \pm 0.055 \text{ kg/m}^3$

(0.017% ± 0.008%). A complementary analysis allowed quantifying the retention decrease to  $1.279 \pm 0.702 \text{ kg/m}^3$  (1.53% ± 0.84%) after keeping the samples at 35 °C, for 3 h.

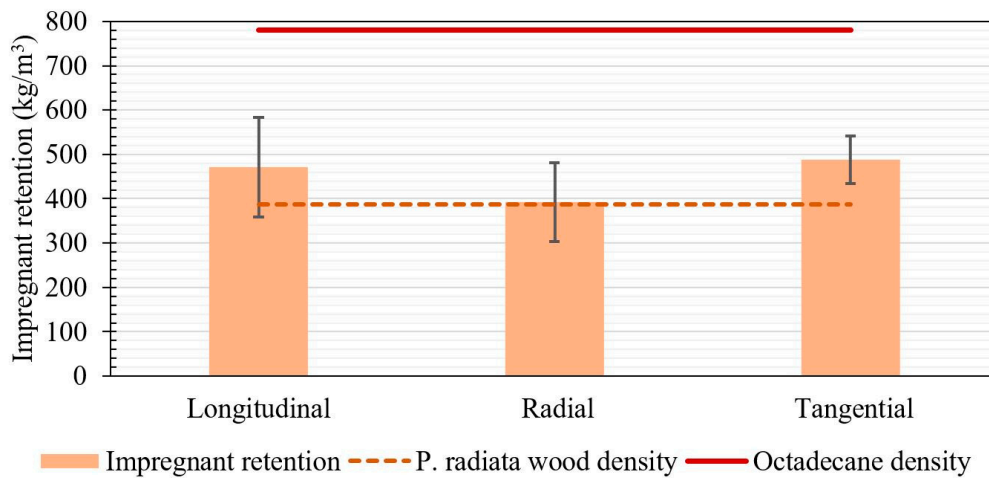


**Figure 7.** Retention of wood samples after impregnation with octadecane.

### 3.2. Evaluation of the Proposed Experimental Setup

Figure 8 shows the behavior of the thermal conductivity and the temperature of tangential samples of impregnated wood as a function of time, using the setup of Figure 4. According to measurements made, it is seen that the thermal conductivity succeeded in stabilizing each temperature level, a behavior observed in samples, in all directions. In the temperature range with PCM in the solid phase (5–20 °C), the thermal conductivity shows an increasing performance with temperature (Figure 8b). In the temperature range with PCM in the liquid phase (30–35 °C), the conductivity remained practically constant to temperature changes (Figure 8c). In the transition region (20–26 °C), the conductivity increased considerably, giving to thermal conductivity transient curve a discontinuous behavior during the heating process (Figure 8a). The method for determining the thermal properties, using a dual needle probe, is based on the analytical solution for transient problem of instantaneous linear source of heat [26,27]. Through this method, one probe emits heat and the other measures the temperature as a function of time so that, at  $r = 0$ , there is a constant instantaneous heat flux, and at  $r \rightarrow \infty$  the temperature is considered constant ( $T = T_0$ ), as seen in Figure 9a. The analytical solution of this problem can be approximate by the following equation [28], considering only the few first terms of the summation solution:

$$T(t) - T_0 = \frac{qb_0 t}{4\pi} + \frac{qb_1}{4\pi} E_i\left(\frac{b_2}{t}\right), \quad (2)$$

where the thermal properties are obtained from the constants ( $b_1 = 1/k$  and  $b_2 = r^2/4\alpha$ ). However in this case, there is a process of fusion of PCM incorporated within the wood porous matrix; so there is a mobile border between liquid and solid phases, whose position is time dependent (Figure 9b). For this reason, the boundary condition must be modified to  $r = r_0$  at the solid–liquid interface  $x(t)$ , where the solid (s) and liquid (l) phases are in thermal equilibrium ( $T_s = T_l$ ). The position of the solid–liquid interface  $x(t)$  requires an additional equation that depends, in this case, from the latent heat of fusion [29]:

$$k_s \frac{\partial T_s}{\partial r} - k_l \frac{\partial T_l}{\partial r} = \rho h_{ls} \frac{\partial x}{\partial t}. \quad (3)$$

The proper thermal conductivity behavior interpretation at the phase change region depends on the solution of the transient line heat source problem considering the phase change and the movement of the liquid front. Although the solution to this problem is interesting, it is beyond the scope of this work.

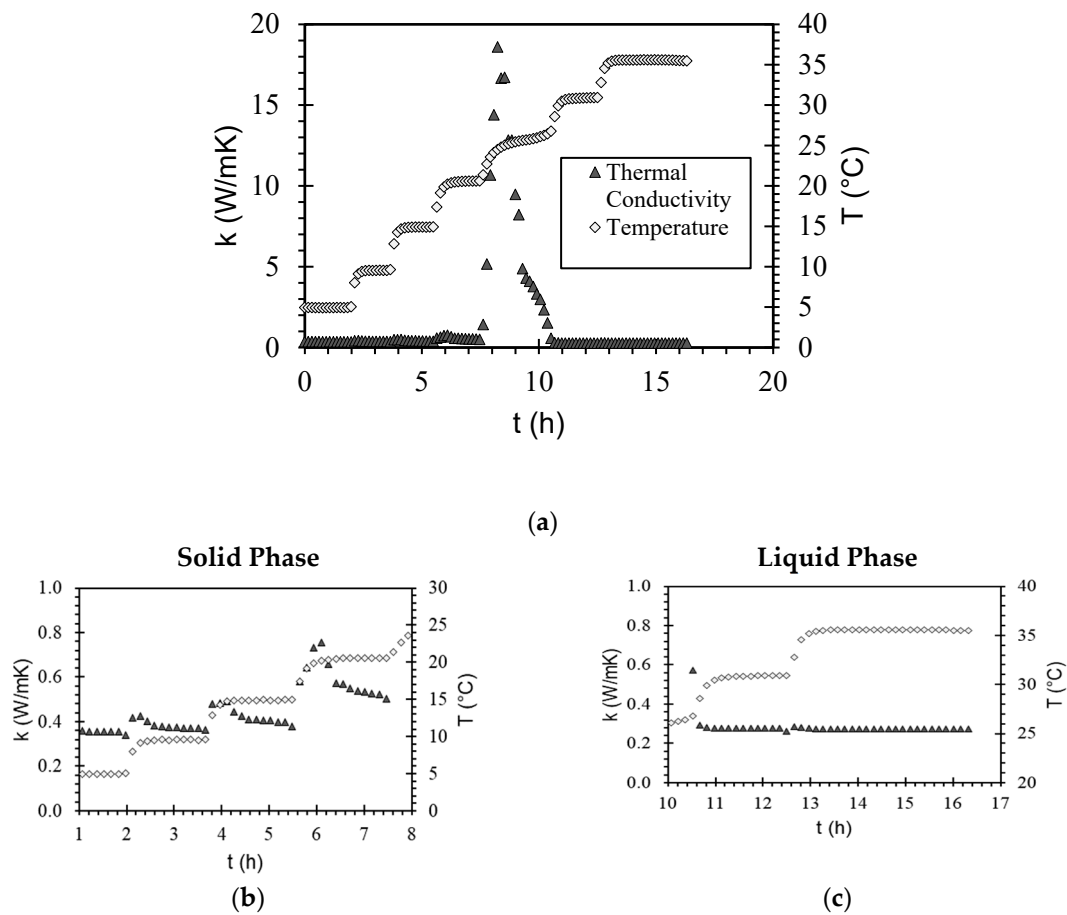


**Figure 8.** (a) Behavior of the thermal conductivity of impregnated wood sample (tangential cut) as a function of time and temperature: (b) solid phase details and (c) liquid phase details.

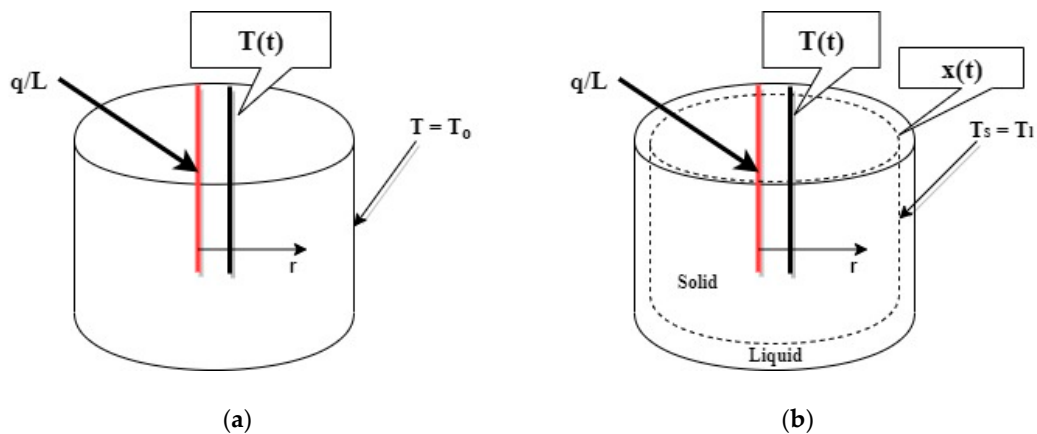


**Figure 9.** Conduction of transient line heat source physical situation problem (a) without phase change and (b) with phase change.

Temperature and humidity records in the test vessel are presented in Figure 10. One can see that during the vessel sealing with plastic film, both the temperature and humidity decreased rapidly, the former from the heat exchange with the double wall glass vessel that is at 5 °C, and the latter by moisture absorption by the silica gel. Furthermore, one can see that the temperature of the vessel was increasing due to thermal equilibrium stages, with the help of the thermoregulated device, achieving seven temperature levels. In the case of humidity, one can see, that after the initial abrupt decrease, it later increased due to the subsequent evaporation of the condensate that initially was formed on the

surfaces of the hoses and the double-walled vessel, and then the relative humidity was dampened by moisture absorption by silica gel. Finally, the vessel was opened for sample change, and the relative humidity increased, becoming equal to that of the laboratory.

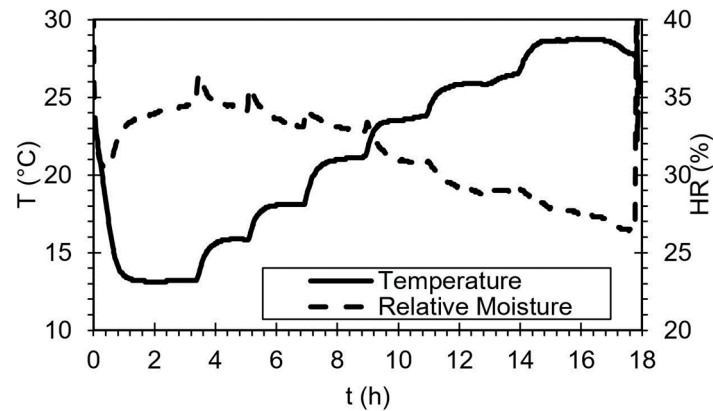


**Figure 10.** Temperature and relative humidity vessel behavior as a function of time during wood sample test in the tangential direction.

### 3.3. Thermal Characterization of the Wood Impregnated with PCM

During the melting period, PCM stores part of the heat released by one of the needles of the probe, and during the cooling period, PCM releases the stored heat by increasing the temperature of the second needle, resulting in the modification of adjustment parameters curve; so during the PCM transition phase, thermal conductivity values increased significantly. Although the thermal conductivity measured during the transition phase was not valid, the technique for measuring this property was able to capture transition phase changes of PCM embedded in *Pinus radiata* wood. Thermal conductivity and specific heat of octadecane and *Pinus radiata* wood, with and without impregnation, and for the three anatomical directions (longitudinal, radial and tangential) are presented as a function of the temperature in Figures 11 and 12, respectively. Both *Pinus radiata* wood thermal conductivity and specific heat did not vary considerably in the temperature range analyzed (5–35 °C). For this reason, the values of conductivity and specific heat are represented by two horizontal lines, showing the lower limit (average value minus standard deviation) and the upper limit (average value plus standard deviation) of these properties, according to the direction.

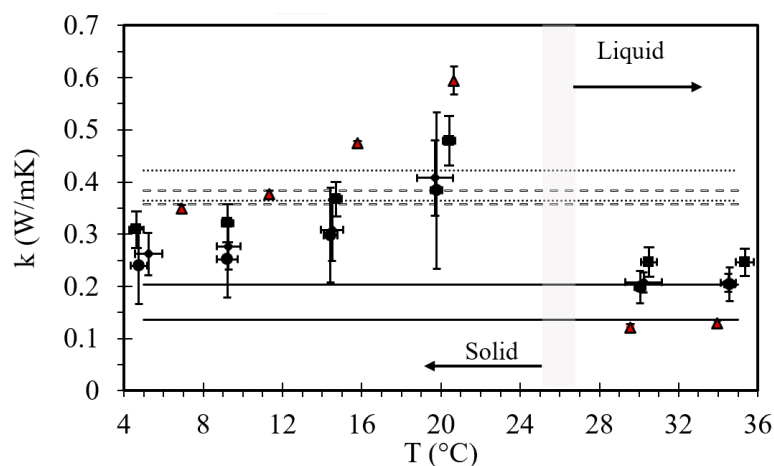


**Figure 11.** *Pinus radiata* wood impregnated with octadecane thermal conductivity (longitudinal: rhombus; tangential: square and radial: circle) of the unimpregnated wood (longitudinal: solid line; tangential: dashed line and radial: dotted line), and of octadecane (red triangle).

Figure 11 shows *Pinus radiata* wood thermal conductivity behavior in its three anatomical directions. When PCM was in the solid phase, the ANOVA analysis, performed using the Open Source RStudio 1.2.5019 software, indicates that there was no statistically significant difference ( $\alpha = 0.05$ ) between the mean thermal conductivities of wood samples impregnated in longitudinal and tangential directions against those corresponding to longitudinal and radial directions. The high dispersion of thermal conductivity measurements in the tangential and radial directions did not allow a comparative ANOVA analysis. With respect to octadecane, one can see that thermal conductivity behavior in its solid phase was not linear with temperature, but adjustable to a second degree polynomial. In the liquid phase thermal conductivity decreased and was practically constant in the temperature range 30–35 °C. Impregnated wood thermal conductivity had a behavior similar to octadecane in the three anatomical directions, also was adjustable to a second degree polynomial at the solid temperature phase range (5–20 °C) and was practically constant in the temperature range where PCM was in the liquid phase. Furthermore, one can see that measurements dispersion increased with temperature, and this could be explained by the mobility of molten PCM in the porous matrix of the wood.

When PCM was in the liquid state, the ANOVA analysis indicates that there were statistically significant differences between thermal conductivities recorded in the longitudinal and tangential directions ( $\alpha = 0.05$ ), with respect to thermal conductivity, being higher in the tangential direction. On the other hand, there were no significant differences in thermal conductivity between longitudinal and radial directions. Finally, tangential direction had a higher thermal conductivity than the radial direction at 30 °C; however, at 35 °C there were no statistically significant differences. In general, impregnated wood thermal conductivity could be considered to vary from 0.20 to 0.25 W/mK at temperatures between 30 and 35 °C.

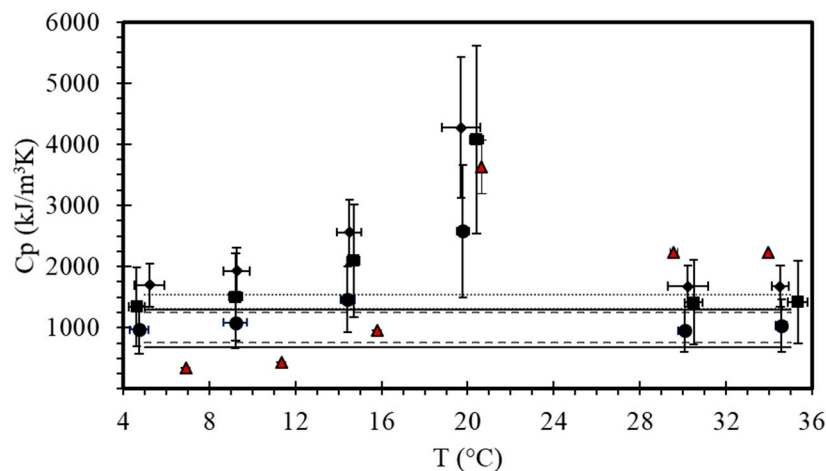


**Figure 12.** Volumetric specific heat of *Pinus radiata* wood impregnated with octadecane (longitudinal: rhombus; tangential: square and radial: circle), of the unimpregnated wood (longitudinal: solid line; tangential: dashed line and radial: dotted line) and octadecane (red triangle).

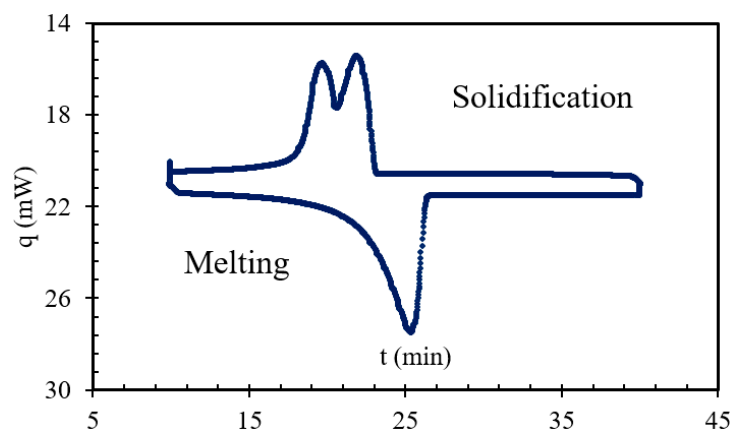
The volumetric specific heat of wood with and without impregnation and of PCM are presented in Figure 12. The volumetric specific heat of *Pinus radiata* wood did not show significant variations in the temperature range studied. The ANOVA analysis indicates that there were no statistically significant differences ( $\alpha = 0.05$ ) of the specific heat in between the three directions. The behavior of the octadecane specific heat with temperature was adjusted to a third degree polynomial. Furthermore, it is seen that the specific heat of the impregnated wood had a nonlinear behavior with temperature, being well described by a second degree polynomial for the three directions of the log. According to the results, the specific heat of the modified wood acquired a nonlinear behavior due to the presence of octadecane, finding that the specific heat of the impregnated wood was greater than that of wood at a temperature of 10 °C, keeping the same trend to the maximum specific heat value at 20 °C.

The ANOVA analysis indicates that there were no statistically significant differences ( $\alpha = 0.05$ ) of the average heat capacity values in between the three anatomical directions analyzed, when PCM was in the solid state. Similarly, when PCM was in the liquid phase (30–35 °C), the ANOVA analysis suggests that there were no statistically significant differences ( $\alpha = 0.05$ ) of the mean heat capacity values in between the three directions of the analyzed log.

Regarding unimpregnated *Pinus radiata* wood, the ANOVA analysis indicates that there were no statistically significant differences ( $\alpha = 0.05$ ) of the specific volumetric heat at 20 °C in between the three directions of the log. In general, the thermal conductivity and the heat capacity for unimpregnated wood did not present a significant variation with temperature; so the nonlinear variation of impregnated wood with temperature was explained by the thermal behavior of PCM. It is interesting to note that solid octadecane thermal conductivity was higher than *Pinus radiata* impregnated wood when PCM was in the solid phase; on the contrary, when it was in the liquid phase, octadecane thermal conductivity was lower than that of the impregnated wood. The opposite occurred in the case of the volumetric specific heat: while in the solid phase, this property was higher than that of impregnated wood, in the liquid phase octadecane had a higher heat capacity. The difference in *Pinus radiata* wood thermal conductivity in the longitudinal direction and in the radial and tangential directions was reduced when the wood was impregnated, which might be evidence that impregnation with PCM decreased the orthotropic characteristics of *Pinus radiata* wood. However, it should be considered that impregnation results in a dispersion in measurements of thermal conductivity and volumetric specific heat.

#### 3.4. Phase Change Enthalpy

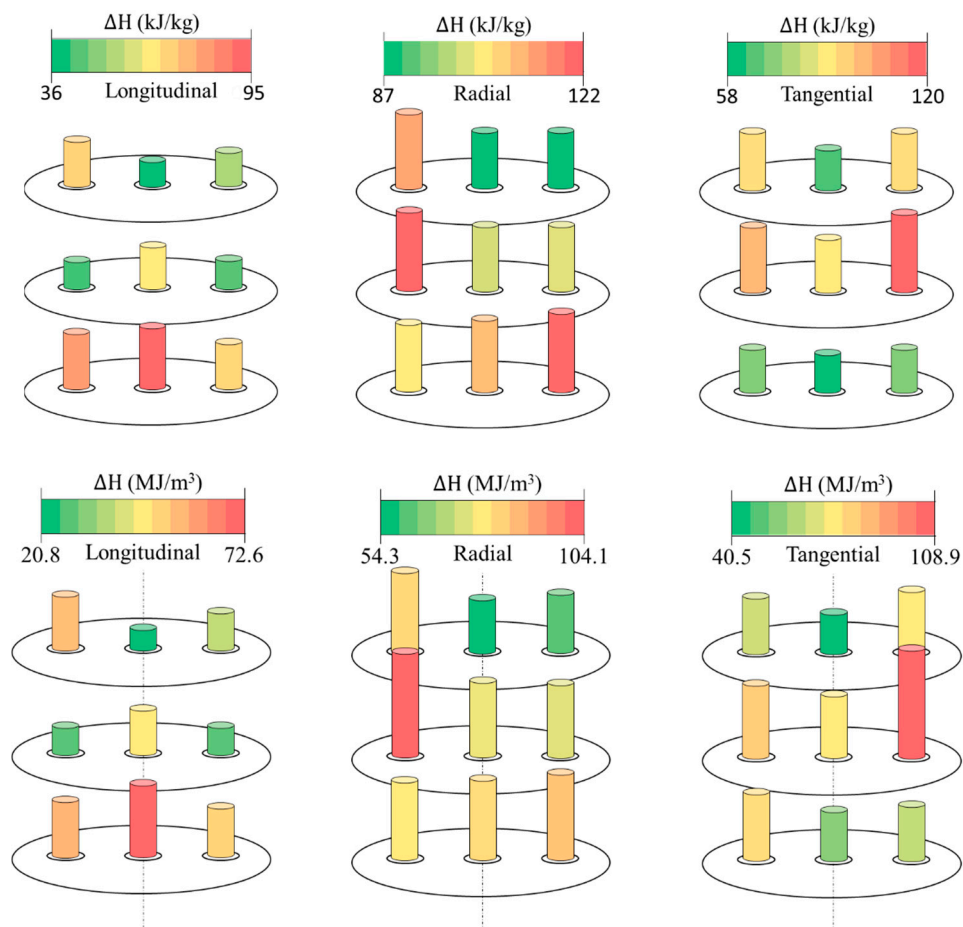
*Pinus radiata* impregnated with PCM samples thermograms obtained by DSC show a maximum heat absorption peak corresponding to melting, and show a maximum double peak of heat release from solidification (Figure 13). This behavior was observed in all samples of different specimens tested, this being an evidence of the impregnation of PCM in the different samples, taken at different points of them (Figure 5).



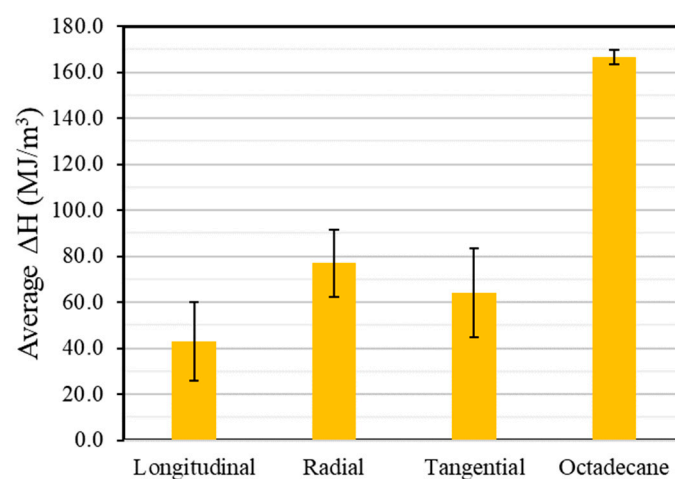
**Figure 13.** DSC analysis: representative response of wood impregnated with PCM.

Figure 14 shows the distribution of the fusion enthalpy for the three anatomical directions analyzed, taking wood samples mass and the approximate volume as a basis. It can be observed that in each position there was a different enthalpy phase change magnitude that shows the heterogeneity of the impregnation. The samples analysis made by DSC on a sample for each direction shows that the radial direction presents a more homogeneous distribution of the capacity to store latent heat than the longitudinal and tangential directions. Figure 15 presents the results of the average phase change enthalpy for three anatomical directions of impregnated wood, and octadecane used as impregnant. The impregnated wood had phase change enthalpies from 23.8% to 49.9% from melting enthalpy of octadecane for longitudinal and radial directions, respectively. It is important to mention that the

volume of the samples was obtained by using the weights and the approximate volume of each sample, assuming that they were discs of uniform shape.



**Figure 14.** Distribution of the latent heat at different positions for wood samples impregnated with octadecane.



**Figure 15.** *Pinus radiata* wood impregnated with octadecane average fusion enthalpy.

The procedure for obtaining impregnated wood samples for the DSC analysis involved a method for reducing the thickness of samples by friction, to adapt the samples dimensions to the crucibles (0.5 mm thick). During this process, heat was generated; so PCM percolation into the samples under

testing occurs. For this reason, measured fusion enthalpy values were lower than those actually obtained by the impregnated specimens. The same occurred with thermal conductivity and volumetric specific heat properties, the dispersion of the enthalpy phase change results from wood impregnated with octadecane, was due to the non-uniform distribution of octadecane within the porous matrix of the wood.

#### 4. Discussion

Impregnating *Pinus radiata* wood with a phase change material (octadecane) does not imply significant dimensional changes (maximum variation of 0.5% in volume). *P. radiata* wood had a high dimensional stability and retention capacity of PCM with a dimensional variation lower than 0.03% and mass losses of up to 2%, when the temperature was higher than the melting temperature (35 °C). The increase in mass of the impregnated wood with respect to unimpregnated wood varied from a minimum of 80% to a maximum of 150%.

The thermal properties of the wood impregnated with temperature acquired the same behavior of those of the impregnant. In PCM solid region (5–20 °C), thermal conductivity and volumetric heat capacity were adjustable to a second-degree polynomial. In the transition region, the transient line heat source method could record the phase change phenomenon, but thermal conductivity values obtained in this region had no physical meaning. In PCM liquid region (30–35 °C), thermal conductivity and volumetric specific heat remained constant, and were smaller in magnitude as compared to those measured in PCM solid region. Velez et al. [30] observed similar trends of the behavior of both thermal conductivity and heat capacity for reactive grade octadecane. *Pinus radiata* wood in the tangential and radial directions does not show statistically significant differences (ANOVA,  $\alpha = 0.05$ ) in their thermal conductivity averages. A different behavior was observed by Vay et al. [31], who found that longitudinal thermal conductivity of three different wood species (European oak, European beech and Norway spruce) is higher. Thermal conductivity of the impregnated wood in both tangential and radial directions were higher than that measured for the longitudinal direction at 20 °C.

By impregnating *Pinus radiata* wood with octadecane, the anisotropic behavior of thermal conductivity was altered according to the phase in which the PCM was found. For the PCM solid region, average thermal conductivity did not show statistically significant differences in between longitudinal and tangential, and longitudinal and radial directions. In the PCM liquid region, there were no statistically significant differences in thermal conductivity between longitudinal and tangential directions. Tangential and radial directions did not show statistically significant differences at 35 °C, but they did at 30 °C, where thermal conductivity was higher in the tangential direction. *Pinus radiata* wood anatomical direction did not affect in a significant way ( $\alpha = 0.05$ ), the mean volumetric specific heat value, even when the wood was impregnated with PCM.

Volumetric specific heat did not present statistically significant differences (ANOVA,  $\alpha = 0.05$ ) in the three anatomical directions when PCM was in the solid or in the liquid regions. Therefore, impregnation with octadecane did not affect the isotropic behavior of *Pinus radiata* wood specific heat.

Impregnation with octadecane increases *Pinus radiata* wood specific heat in the temperature range 15–20 °C. At higher temperatures, the heat capacity decreased, approaching to that of *Pinus radiata* wood without impregnation. Although, the longitudinal direction thermal conductivity increased with the impregnation, radial and tangential direction thermal conductivity decreased as compared to unimpregnated wood, with the exception of 20 °C, where both directions exceeded *Pinus radiata* without impregnation thermal conductivity.

The DSC analysis shows the heterogeneity of PCM impregnation through the porous matrix of *Pinus radiata* wood, with the latent heat presenting a stable (repetitive) response during PCM melting and solidification. Fusion enthalpy varied from 26.8% to 49.9% with respect to octadecane fusion enthalpy. These values were considered conservative, given the loss of PCM in the analyzed samples, due to the sample extraction and preparation method.

This paper was limited to the study of the thermal properties of *Pinus radiata* wood impregnated with octadecane depending on the temperature and the anatomical orientation. The behavior of the composite material with moisture is not explicit, so in later studies, one recommended to analyze the effect of humidity. Moreover, the low thermal conductivity of both PCM and wood might be an issue in a practical application during building temperature cycles. Therefore, it could be considered a drawback during the charging/discharging process of the shape-stabilized PCM. This is a subject that should be addressed in a future study.

## 5. Conclusions

In general, the impregnation of *Pinus radiata* wood with octadecane did not change its dimensions, and despite the nonpolar character of the impregnant, the wood had a good retention capacity. The octadecane is distributed in a non-homogeneous way in the porous network of the wood, which anyway acquires the ability to store latent heat. Due to the impregnation, a reduction in the difference in thermal conductivity between the anatomical orientations was also found, maintaining the isotropic behavior of specific heat. In this way, the potential of the composite material in latent heat storage systems was demonstrated. However, tests on flammability, phenomenological study at a pore size scale and effects of wood type analysis (central, lateral, early or late, sapwood and heartwood) are required.

**Author Contributions:** Conceptualization, R.F.-S. and D.A.V.; methodology, R.F.-S. and D.A.V.; resources, C.S.-L. and R.A.A.; data curation, R.F.-S.; writing—original draft preparation, R.F.-S. and D.A.V.; writing—review and editing, C.G.-H., C.S.-L. and R.A.A.; supervision, D.A.V. and C.S.-L.; project administration and funding acquisition D.A.V. All authors have read and agreed to the published version of the manuscript.

**Funding:** Dirección de Investigación, Científica y Tecnológica, Dicyt, Universidad de Santiago de Chile: 051816VC. Dirección de Investigación, Universidad del Bio-Bio, Concepcion, Chile.

**Acknowledgments:** The authors acknowledge the support given by Laboratorio de Ingeniería de Procesos de Alimentos del Departamento de Ciencias de los Alimentos y Tecnología Química, Universidad de Chile.

**Conflicts of Interest:** The authors declare no conflict of interest.

## References

1. Anuario Estadístico de Energía 2018. Available online: <https://www.cne.cl/wp-content/uploads/2019/04/Anuario-CNE-2018.pdf> (accessed on 11 November 2019).
2. Calificación Energética de Viviendas. Available online: <https://www.calificacionenergetica.cl/media/CEV-2014.pdf> (accessed on 11 November 2019).
3. Estudio de Usos Finales y Curva de Oferta de la Conservación de la Energía en el Sector Residencial. Available online: [http://dataset.cne.cl/Energia\\_Abierta/Estudios/Minerg/Usos%20finales%20y%20curva%20de%20oferta%20de%20conservaci%C3%B3n%20de%20la%20energ%C3%ADa%20en%20el%20sector%20de%20residencial%20de%20Chile.pdf](http://dataset.cne.cl/Energia_Abierta/Estudios/Minerg/Usos%20finales%20y%20curva%20de%20oferta%20de%20conservaci%C3%B3n%20de%20la%20energ%C3%ADa%20en%20el%20sector%20de%20residencial%20de%20Chile.pdf) (accessed on 11 November 2019).
4. Política de Uso de la Leña y Sus Derivados Para Calefacción. Available online: [http://www.minenergia.cl/archivos\\_bajar/2016/03/politica\\_leña\\_2016\\_web.pdf](http://www.minenergia.cl/archivos_bajar/2016/03/politica_leña_2016_web.pdf) (accessed on 11 November 2019).
5. The Industry-Driven Initiative on Advanced Materials for Low Carbon Energy Technologies, EMIRI. 2016. Available online: [https://emiri.eu/news\\_and\\_documents](https://emiri.eu/news_and_documents) (accessed on 8 November 2019).
6. Hawes, D.W.; Feldman, D.; Banu, D. Latent heat storage in building materials. *Energy Build.* **1993**, *20*, 77–86. [[CrossRef](#)]
7. Elnajjar, E. Using PCM embedded in building material for thermal management: Performance assessment study. *Energy Build.* **2017**, *151*, 28–34. [[CrossRef](#)]
8. Silva, T.; Vicente, R.; Rodrigues, F. Literature review on the use of phase change materials in glazing and shading solutions. *Renew. Sustain. Energy Rev.* **2016**, *53*, 515–535. [[CrossRef](#)]
9. Kośny, J. *PCM-Enhanced Building Components*, 1st ed.; Derby, B., Ed.; Springer: Berlin/Heidelberg, Germany, 2015; ISBN 978-3-319-14285-2.
10. INFOR La Industria del Aserrío. 2018. Boletín Estadístico 165. Available online: <https://www.infor.cl/index.php/destacados-home/486-la-industria-del-aserrio-2017-boletin-n-161> (accessed on 8 November 2019).

11. Promoviendo el Uso de la Madera en Chile. Available online: <http://www.emb.cl/construccion/articulo.mvc?xid=2457&tip=1&xit=promoviendo-el-uso-de-la-madera-en-chile> (accessed on 8 November 2019).
12. INE. Edificación: Informe Anual 2016. Available online: <https://www.ine.cl/docs/default-source/publicaciones/2017/informe-anual-de-edificaci%C3%B3n-2016.pdf?sfvrsn=5> (accessed on 8 November 2019).
13. Zenteno, F.V. Situación Actual de la Madera en Chile en el Contexto de la Construcción en Edificación. Master's Thesis, Universidad Mayor, Santiago, Chile, 2017.
14. NCH433 Clasificación Estructural de la Madera. Available online: <https://es.slideshare.net/randysreyman/norma-chilena-nch4331996-mod2009> (accessed on 8 November 2019).
15. Salvo, L.; Ananías, R.; Cloutier, A. Influencia de la estructura anatómica de la permeabilidad específica transversal al gas del Pino radiata. *Maderas Cienc. Tecnol.* **2004**, *6*, 33–44.
16. Kininmonth, J.A.; Whitehouse, L.J. *Properties and Uses of New Zealand Radiata Pine. Volume 1, Wood Properties*; New Zealand Ministry of Forestry, Forest Research Institute: Wellington, New Zealand, 1991; ISBN 0473011816.
17. Li, Y.; Li, X.; Liu, D.; Cheng, X.; He, X.; Wu, Y.; Li, X.; Huang, Q. Fabrication and Properties of Polyethylene Glycol-Modified Wood Composite for Energy Storage and Conversion. *BioResources* **2016**, *11*, 7790–7802. [[CrossRef](#)]
18. Barreneche, C.; Vecstaudza, J.; Bajare, D.; Fernandez, A.I. PCM/wood composite to store thermal energy in passive building envelopes. *IOP Conf. Ser. Mater. Sci. Eng.* **2017**, *251*, 12111. [[CrossRef](#)]
19. Vasco, D.A.; Salinas-Lira, C.; Barra-Reyes, I.; Elustondo, D.M. Kinematic characterization of the pressure-dependent PCM impregnation process for radiata pine wood samples. *Eur. J. Wood Wood Prod.* **2018**, *76*, 1461–1469. [[CrossRef](#)]
20. Mathis, D.; Blanchet, P.; Landry, V.; Lagièrre, P. Impregnation of wood with microencapsulated bio-based phase change materials for high thermal mass engineered wood flooring. *Appl. Sci.* **2018**, *8*, 2696. [[CrossRef](#)]
21. Montanari, C.; Li, Y.; Chen, H.; Yan, M.; Berglund, L.A. Transparent Wood for Thermal Energy Storage and Reversible Optical Transmittance. *ACS Appl. Mater. Interfaces* **2019**, *11*, 20465–20472. [[CrossRef](#)] [[PubMed](#)]
22. Petr, P.; Aleš, D. Moisture absorption and dimensional stability of poplar wood impregnated with sucrose and sodium chloride. *Maderas Cienc. Tecnol.* **2014**, *16*, 299–311.
23. Gute Chemie. Available online: <https://www.abcr.de/> (accessed on 11 November 2019).
24. Listado de Normas Técnicas Obligatorias. Available online: <http://normastecnicas.minvu.cl/> (accessed on 8 November 2019).
25. Lazaro, A.; Peñalosa, C.; Solé, A.; Diarce, G.; Haussmann, T.; Fois, M.; Zalba, B.; Gshwander, S.; Cabeza, L.F. Intercomparative tests on phase change materials characterisation with differential scanning calorimeter. *Appl. Energy* **2013**, *2013*, 415–420. [[CrossRef](#)]
26. De Vries, D.A. A nonstationary method for determining thermal conductivity of soil in situ. *Soil Sci.* **1952**, *73*, 83–89. [[CrossRef](#)]
27. Kluitenberg, G.J.; Bristow, K.L.; Das, B.S. Error analysis of heat pulse method for measuring soil heat capacity, diffusivity, and conductivity. *Soil Sci. Soc. Am. J.* **1995**, *59*, 719–726. [[CrossRef](#)]
28. KD2 Pro Thermal Properties Analyzer. Available online: [http://manuals.decagon.com/Manuals/13351\\_KD2Pro\\_Web.pdf](http://manuals.decagon.com/Manuals/13351_KD2Pro_Web.pdf) (accessed on 8 November 2019).
29. Jaeger, J.C.; Carslaw, H.S. *Conduction of Heat in Solids*, 2nd ed.; Press, O.U., Ed.; Springer: Berlin/Heidelberg, Germany, 1986; ISBN 0198533683.
30. Vélez, C.; Khayet, M.; De Zárte, J.O. Temperature-dependent thermal properties of solid/liquid phase change even-numbered n-alkanes: N-Hexane, n-octadecane and n-eicosane. *Appl. Energy* **2015**, *143*, 383–394. [[CrossRef](#)]
31. Vay, O.; De Borst, K.; Hansmann, C.; Teischinger, A.; Müller, U. Thermal conductivity of wood at angles to the principal anatomical directions. *Wood Sci. Technol.* **2015**, *49*, 577–589. [[CrossRef](#)]

